J. Serb. Chem. Soc. 72 (8–9) 833–846 (2007)
JSCS–3616
UDC 547.221:536.2:536.7:536.423.1
Original scientific paper

Mean heat transfer coefficients during the evaporation of 1,1,1,2-tetrafluoroethane (R-134a) in a plate heat exchanger

EMILA DJORDJEVIĆ[1]*#, STEPHAN KABELAC[2] and SLOBODAN ŠERBANOVIĆ[1#]

[1]*Faculty of Technology and Metallurgy, University of Belgrade, Karnegijeva 4, 11120 Belgrade, Serbia and* [2]*Helmut Schmidt University of Federal Armed Forces, Holstenhofweg 85, D–22043 Hamburg, Germany*

(Received 8 February 2007)

Abstract: In this study the transfer coefficient of evaporation heat of the refrigerant 1,1,1,2-tetrafluoroethane (R-134a) in a vertical plate heat exchanger was experimentally investigated. The results are presented as the dependancy of the mean heat transfer coefficient for the whole heat exchanger on the mean vapor quality. The influences of mass flux, heat flux and flow configuration on the heat transfer coefficient were also taken into account and a comparison with previously published experimental data and literature correlations was made.

Keywords: plate heat exchanger, evaporation, 1,1,1,2-tetrafluoroethane, heat transfer coefficient.

INTRODUCTION

In the last decades, one of the applications of the plate heat exchangers has been as evaporators or condensers in many refrigeration, air conditioning and heat pump systems when the fluid acting as a heat source or heat sink was a liquid. This is due to their high thermal performance and compactness. For these purposes various chlorofluorocarbon (CFC) and hydrochlorofluorocarbon (HCFC) refrigerants were used as working fluids. However, due to the serious depletion of the ozone layer in the atmosphere and global warming problems, the use of CFC refrigerants was forbidden and the same destiny is soon awaiting the most extensively used HCFC refrigerant R-22.

As replacements, various new refrigerants, such as R-134a, R-143a, R-125, R-410a, R-410b, R-507 have been developed during the past years, which necessitates knowledge of their thermodynamic, thermophysical and heat transfer properties.

Moreover, better comprehension of the heat transfer characteristics during evaporation and condensation of the new refrigerants is also essential for the design of evaporators and condensers.

* Corresponding author. E-mail: emila@tmf.bg.ac.yu
# Serbian Chemical Society member.
doi: 10.2298/JSC0709833D

The available literature data on two-phase heat transfer, especially for the new refrigerants in plate heat exchangers, are relatively scarce. In the past few years some experimental data have been published the evaporation and condensation of R-134a and R-410a in a vertical plate heat exchanger.[1–6] Evaporation of ammonia[7] and R-22[8] has also been the subject of experimental investigation. Previously, heat transfer during the boiling process had been investigated on different plate geometries, with several refrigerants (R-12, R-22, R-113 and R-717) being used as working fluids.[9]

Several studies have been published on the heat transfer during evaporation and condensation of the refrigerant R-22 in micro-fin tubes of various outer diameter.[10–12] Also, heat transfer during evaporation and condensation inside horizontal smooth tubes has been examined for a series of refrigerants, including R-12 and R-134a,[13] and R-22, R-410a and R-407c.[14,15]

A short literature review of previous investigations on boiling or evaporation of different refrigerants in plate heat exchangers is given in Table I.

TABLE I. Previous investigations of evaporation or boiling in a plate heat exchangers

Ref.	Substance	Plate type	Mass flux kg $m^{-2}s^{-1}$	Heat flux or heat rate
1	R-134a	Herringbone type PHE	55, 70	11 and 15 kW m^{-2}
3	R134-a	Herringbone type PHE	50–200	0–35
4	R-410a	Herringbone type PHE	50–100	10 and 20 kW m^{-2}
6	R-410a	Herringbone type PHE	50–125	5–35 kW m^{-2}
16	NH_3	Herringbone type PHE	9–25	10–30 kW m^{-2}
9	R-22, R-12, R-113, R-717	Herringbone type PHE	–	1–20 kW m^{-2} 0.3–23 kW m^{-2} 1.5–17 kW m^{-2}
23	R-22, R-134a, R-134a/R-32, R-134a/R-125/R-134a	Semi-welded PHE, Nickel-brazed PHE	50–200	12–20 kW
7	NH_3	Herringbone type PHE	0.5–9.5	12–185 kW
8	R-22	Herringbone type PHE with enhanced surfaces	25.5–36.3	14.7–21.9 kW m^{-2}

The experimental system used in the present investigation includes two vertical plate heat exchangers – an evaporator and a condenser. The experiments were conducted under various test conditions – temperature, pressure and volume flow rate, employing the refrigerant R-134a. The collected data enabled the calculation of both the mean and local values of the heat transfer coefficients, as well as the pressure drops in the plate heat exchangers. In the study presented here, focus was directed on an experimental investigation of heat transfer and pressure drop of the refrigerant R-134a in the evaporator.

EXPERIMENTAL

The experimental system (Fig. 1) was used to investigate the evaporation and condensation of the refrigerant R-134a in a vertical plate heat exchanger (PHE). It includes two main loops – a refrigerant loop and a water–glycol loop, as well as a data acquisition unit.

During the experiments, the temperatures, pressures and flow rates were measured in both loops.

Refrigerant loop

The refrigerant loop contains an evaporator (1), a separation vessel (2), an expansion valve (3), an inner heat exchanger (4), a compressor (5), two oil separators (6), a condenser (7), a refrigerant collector with level indicator (8), two sight glasses and two volume flowmeters, one at the evaporator inlet and the other just before the expansion valve.

A vertical plate and frame heat exchanger is used as the evaporator (1). A liquid refrigerant enters the evaporator at a temperature just a few degrees below the saturation point. In order to obtain various test conditions of R-134a, especially the vapor quality at the exit, pressure, flow rate and imposed heat flux, various water–glycol flow rates were used and the compressor power was changed. It is also possible to investigate the influence of flow direction on heat transfer and pressure drop by changing the direction of the water–glycol flow from concurrent to countercurrent with a four-way valve (9). The flow direction of the refrigerant is always bottom up.

After partial evaporation in the plate heat exchanger, the two-phase refrigerant flow enters the separator (2). The liquid part is collected at the bottom of the vessel, together with the liquid fraction behind the expansion valve and directed back to the evaporator. The volume flow rate in this inner cycle is measured at the evaporator inlet by a calibrated Krohne Ultrasonic Flowmeter (type UFM 3030) with an accuracy of ±1 %. Vapor from the top of the vessel is superheated in the double-pipe inner heat exchanger (4) by heat transfer from the "hot" liquid refrigerant flowing on the other side.

After the heat exchanger, the superheated R-134a vapor passes through a compressor (5) and oil separators (6) before entering the condenser (7). In this set-up, a Bock F16/2051 compressor is used, which offers the choice of working with two, four or with all six cylinders, thus achieving different pressures and flow rates of the refrigerant. A detailed investigation was performed[16] in order to check the efficiency of the used oil separators. Typically the oil content behind the separators was less than 0.2 mass %.

Another vertical plate heat exchanger functions as a countercurrent flow condenser (7). The superheated refrigerant vapor, which enters the condenser at the top, is completely condensed by the time it reaches the bottom and exits as a sub-cooled liquid. The water–glycol mixture passes through the condenser in the opposite direction, from bottom to top.

From the condenser, the liquid R-134a first flowed to the collector vessel (8), where the liquid level was constant during stationary operation, visually monitored on a sight glass and measured by the level indicator, and then to the inner heat exchanger (4) and the expansion valve (3). After reduction of the pressure, so that partial evaporation occurs in the expansion valve, the two-phase refrigerant flow enters the separation vessel (2), where the cycle is completed.

Before the expansion valve, the volume flow rate of R-134a was measured again by a turbine flow meter, thus enabling the overall energy balance for the refrigerant loop to be checked and the vapor qualities after expansion and evaporation calculated. Additionally, energy balances were calculated for the evaporator and the condenser, as separate units, using both the refrigerant and the water–glycol side. The results showed good agreement between the energy input and output (less than 2 % difference) for all cases reported here.

For temperature measurement, Pt100 thermometers are situated in the middle of the flow, at the evaporator inlet and outlet, the condenser inlet and outlet, the compressor inlet and outlet and in front of the expansion valve. The pressure in the system is measured by two types of pressure transducers – with measuring ranges 0–10 bar and 0–16 bar and a measuring accuracy of ±0.5 %.

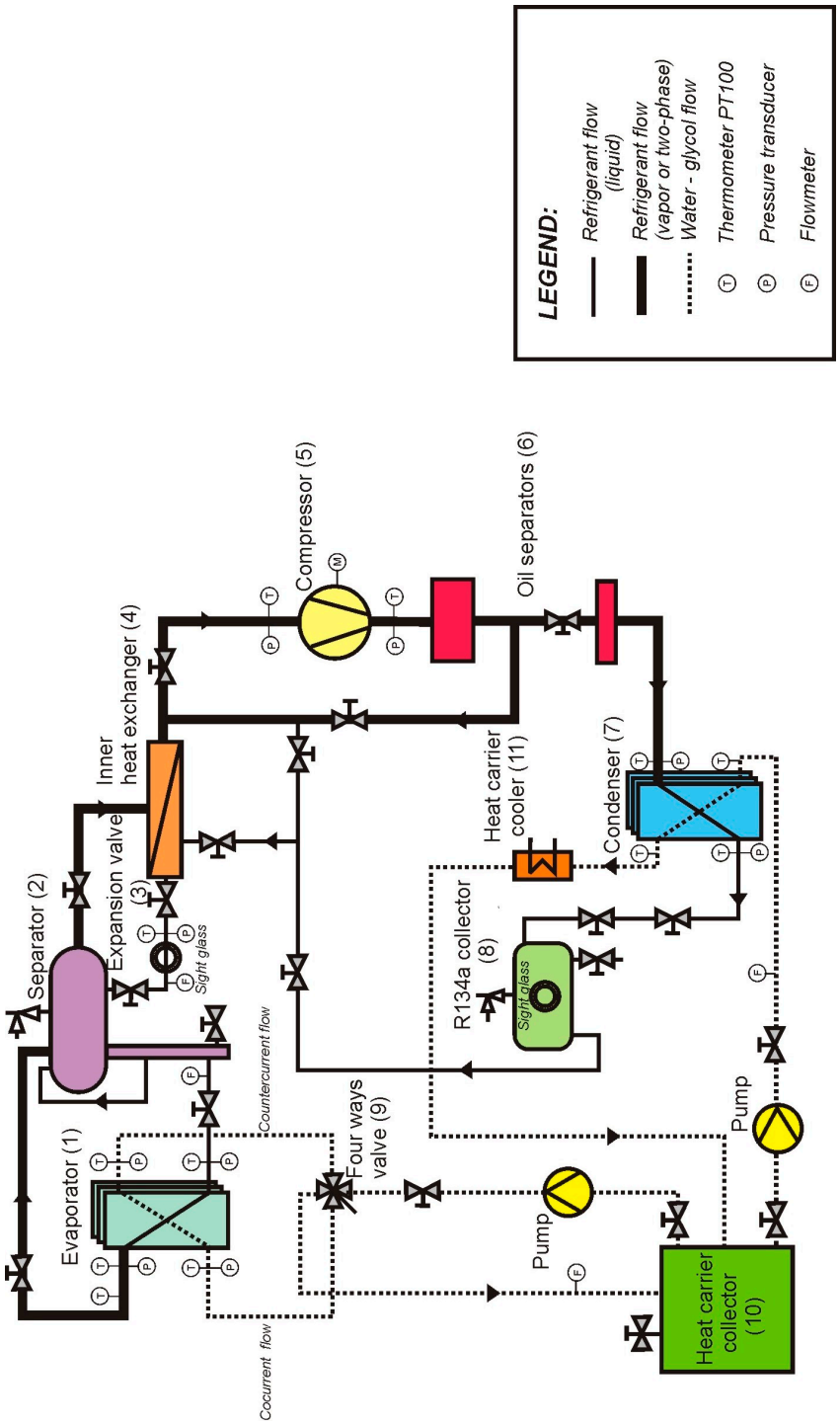

Fig. 1. Experimental setup.

Water–glycol loop

The water–glycol loop consists of two sub-cycles, one connected with the evaporator and the other with the condenser. A mixture with 30.6 mass % of glycol is transported from the heat carrier collector (10) to the plate heat exchangers by flow regulated pumps. After passing through the evaporator in either concurrent or countercurrent flow, the cooled water–glycol mixture returns to the tank. In the condenser, sub-cycled hot water–glycol flow is partially cooled with external cooling water in a brazed plate heat exchanger (11) (type Gea Ecobraze AB) and then returned to the tank. This external cooling compensates the energy input from the compressor so as to keep the overall setup in a stationary state.

For temperature measurement of the heating/cooling fluid, at the inlets and outlets of both heat exchangers, Pt100 thermometers are used, while the pressure is measured by pressure transducers having a measurement range of 0–4 bar and an accuracy of ±0.5 %. The flow rate in the evaporator sub-cycle is measured by a turbine flowmeter with an accuracy of ±1.5 % and in the condenser sub-cycle by a Trimec Multipulse Positive Displacement MP025 flowmeter, with an accuracy of ±0.5 %. The resistance thermometers, the pressure transducers and the flow meters were repeatedly calibrated.

Data acquisition

The data acquisition system includes a recorder (Kethley 2750 Multimeter), a power supply and a personal computer. The temperature and voltage data are recorded and the collected data signals are then transmitted through a GPIB interface to a computer for further analysis. The experiment is monitored and controlled, and a preliminary balance check is performed by a routine written in LabVIEW® program.

It usually takes approximately 20 minutes for the system to reach stationary state. During this initial period and during the experiments, the acquisition unit scanns all data channels every 10 or 20 s. For further calculations of the heat transfer coefficients and pressure drop, the mean, time averaged value of the data for each channel is used.

Plate heat exchangers

The plate heat exchangers used in this study are formed by 4 double-plate cassettes (type NT150S) produced by GEA Ecoflex in a frame. The plate characteristics are given in Table II and a schematic representation in Fig. 2.

TABLE II. Plate dimension

Length L_p / mm	872
Width B_p / mm	486
Amplitude a / mm	1.6
Wave length Λ / mm	12
Plate thickness δ_p / mm	0.6
Thermal conductivity λ_p / W m^{-1} K^{-1}	15
Corrugation angle / ^{o}	63.26

Refrigerant flow passes inside the cassettes while the water–glycol mixture flows through the channels formed between the cassettes. As sealing against leakage into the environment, EPDM (Ethylene Propylene Diene Monomer) strips are used, while the inlet and outlet ports are sealed with Neopren (Polychloroprene) strips. Thermocouples (type K, 0.5 mm diameter) are welded along the plate surface, in a vertical line on the two middle cassettes, for local temperature measurement. On one of the plates, the thermocouples are used for measuring the wall temperature and on the other for measuring the fluid temperature, thus enabling direct calculation of local heat transfer coefficients on the water–glycol side. The three thermocouples placed near the central horizontal line of

the plates (position 3 in Fig. 2) measure the temperature in the middle of the plate, but also near the edges, which gives a better insight into the flow distribution.

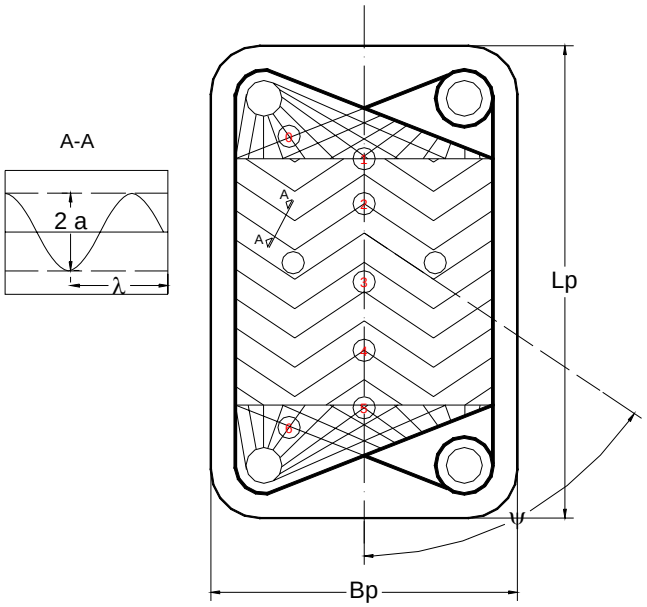

Fig. 2. Geometry of the plates.

Only two thermocouples were installed on each of the two outer cassettes: for measuring the inlet and outlet temperatures, thus enabling a check as to whether the flow distribution between the cassettes is even or not.

Beside measurements by the thermocouples, the temperature of both fluids is measured at the inlet and outlet by Pt100 resistance thermometers, in order to calculate mean heat transfer coefficients. Pressure transducers are also connected to the inlet and outlet of the plate heat exchangers.

Data reduction

Estimation of the mean heat transfer coefficients for the evaporator requires knowledge of the single phase water–glycol heat transfer coefficients. In the course of the analysis, literature correlations, correlation established on the basis of local measurements and a correlation suggested by the plate producer, were used for the calculation of this coefficient and the calculated values were compared.

The overall heat transfer coefficient can be expressed by the equation:

$$U = \frac{Q_\mathrm{h}}{A\Delta T_\mathrm{lmtd}} \tag{1}$$

As the con- or countercurrent flow in the plates was perfect, there was no need for a correction factor in Eq. (1).

The logarithmic mean temperature difference was calculated from the inlet and outlet temperatures of both fluids, measured by Pt100 thermometers:

$$\Delta T_\mathrm{lmtd} = \frac{\Delta T_1 - \Delta T_2}{\ln \dfrac{\Delta T_1}{\Delta T_2}} \tag{2}$$

For the countercurrent flow, the temperature differences are:

$$\Delta T_1 = T_{\mathrm{h,i}} - T_{\mathrm{r,o}}$$
$$\Delta T_2 = T_{\mathrm{h,o}} - T_{\mathrm{r,i}} \tag{3}$$

and for the concurrent flow, these differences can be defined as:

$$\Delta T_1 = T_{\mathrm{h,i}} - T_{\mathrm{r,i}}$$
$$\Delta T_2 = T_{\mathrm{h,o}} - T_{\mathrm{r,o}} \tag{4}$$

where the index h is used for the heating fluid, water/ethylene-glycol mixture and the index r for the refrigerant.

The heat transferred can be calculated from the equation:

$$Q_{\mathrm{h}} = m_{\mathrm{h}}\, c_{p,\mathrm{h}}\, (T_{\mathrm{h,i}} - T_{\mathrm{h,o}}) \tag{5}$$

The available heat transfer area can be expressed as follows:

$$A = 2 L_{\mathrm{p}}\, B_{\mathrm{p}}\, \Phi N \tag{6}$$

where N is the number of cassettes. For a further explanations see the Nomenclature and Fig. 2.

Finally, the mean heat transfer coefficient for the refrigerant can be determined from the following equation in which the fouling resistances are omitted, since the experiments involved new plates with clean surfaces:

$$\frac{1}{\alpha_{\mathrm{r}}} = \frac{1}{U} - \frac{1}{\alpha_{\mathrm{h}}} - \frac{\delta_{\mathrm{p}}}{\lambda_{\mathrm{p}}} \tag{7}$$

The vapor quality at the outlet can be calculated either from the heat transferred in the evaporator:

$$x_{\mathrm{o}} = \frac{1}{\Delta h_v}\left(\frac{Q_{\mathrm{h}}}{m_{\mathrm{r}}} - c_{p,\mathrm{r}}(T_{\mathrm{r}}^{\mathrm{sat}} - T_{\mathrm{r,i}})\right) \tag{8}$$

or from the previously-mentioned overall balance for the refrigerant loop. Agreement between the values calculated by these two approaches was satisfactory, with differences of less than 1 % for all runs. It should be mentioned here that, for the the graphical representation of obtained results given in the Results and Discussion section, instead of the exit value of the vapor quality, the mean vapor quality in the evaporator was used.

Uncertainty analysis was conducted using a formula proposed by Kline and McKlintock.[17] These evaluation results are summarized in TABLE III.

TABLE III. Estimated uncertainties

Parameter	Uncertainty
Geometry of the plates	
Length, width	±0.3 % (max)
Area	±4.5 %
Measuring instruments	
Temperature, PT100	±0.1 °C
Temperature, TC	±0.4 °C
Pressure transducers	±1 %
Water flowrate – turbine	±1.5 %
Water flowrate – multipulse positive displacement flowmeter	±0.5 %
R-134 Flowrate – ultrasonic flowmeter	±1 %
R-134 Flowrate – turbine	±2 %

TABLE III. Continued

Parameter	Uncertainty
Evaporation heat transfer	
Heat flux	±(4–7.5 %)
Vapor quality	±(5–8.5 %)
Evaporation heat transfer coefficient	±(10–15 %)
Friction factor	±(15–17 %)

RESULTS AND DISCUSSION

In the present study of R-134a evaporation in a vertical plate heat exchanger, a series of experiments were conducted under different test conditions.[18] The evaporation temperature was varied from –8.85 to 11.08 °C (saturation pressure from 0.21 to 0.43 MPa), the values of the refrigerant mass flux were between 40 and 90 kg m^{-2} s^{-1} and the imposed heat flux was gradually increased from 9 to 15 kW m^{-2}. The experiments involved both concurrent and countercurrent flow of the fluids through the evaporator. The working conditions of pressure, mass flux, heat flux and flow configuration during the series of experiments discussed in this paper are summarized in Table IV. The thermophysical properties of R-134a necessary for the calculation of the heat transfer coefficient were taken from the REFPROP database.[19] The calculated values of the mean heat transfer coefficient are presented in graphical form in terms of their variation with the mean vapor quality x_m in the plate heat exchanger. The mean vapor quality is defined and calculated as the arithmetic mean value between the inlet and the outlet vapor qualities.

TABLE IV. Working conditions during the experiments

Name	Flow direction	p / MPa	Flux	
			q / kW m^{-2}	m / kg m^{-2} s^{-1}
TEST 1	Concurrent	0.34–0.43	9–11.3	50–60
TEST 1a	Countercurrent	0.34–0.43	9–11.3	50–60
TEST 2	Concurrent	0.34–0.43	9–11.3	60–70
TEST 3	Concurrent	0.34–0.43	9–11.3	70–80
TEST 4	Concurrent	0.34–0.43	9–11.3	80–90
TEST 4a	Countercurrent	0.34–0.43	9–11.3	80–90
TEST 5	Countercurrent	0.26–0.30	11.6–13.5	40–50
TEST 6	Countercurrent	0.26–0.30	11.6–13.5	50–60
TEST 7	Countercurrent	0.26–0.30	11.6–13.5	60–70
TEST 8	Countercurrent	0.26–0.30	13.7–14.9	50–60
TEST 9	Countercurrent	0.26–0.30	13.7–14.9	60–70
Yan	Countercurrent	0.675	11	55 and 70

Previous measurements[1] involving the evaporation of the refrigerant R-134a were conducted in a plate heat exchanger of a smaller size, different geometry, with less single plates and at room temperature (25–31 °C). The results presented

in this study were obtained on a plate heat exchanger with larger number of plates, in order to approach closer the real exploitation conditions, and at lower temperatures. However, a comparison of current data with the earlier values (working conditions under which these values were obtained are also given in Table IV) shows a satisfactory agreement.

In order to calculate the two-phase evaporation heat transfer coefficient, it was necessary to first determine the single-phase values from the local temperature measurements. The results of these measurements are shown in Fig. 3 as a function of Reynolds number. In the final step, the heat transfer coefficients on the single phase, water–glycol mixture, side were correlated using the equation:

$$Nu_{\mathrm{h}} = 0.39515\, Re_{\mathrm{h}}^{0.6244}\, Pr_{\mathrm{h}}^{1/3} \tag{9}$$

while for the calculation of the *Nu* and *Re* numbers, the following definitions were used:

$$Nu_{\mathrm{h}} = \frac{\alpha_{\mathrm{h}} D_{\mathrm{h}}}{\lambda_{\mathrm{h}}} \tag{10}$$

$$Re_{\mathrm{h}} = \frac{\rho_{\mathrm{h}} u_{\mathrm{h}} D_{\mathrm{h}}}{\mu_{\mathrm{h}}} \tag{11}$$

The agreement between the values calculated from the above equations and experimental results is good, having a relative percentage deviation of approximately 2 %, as can be seen in Fig. 3.

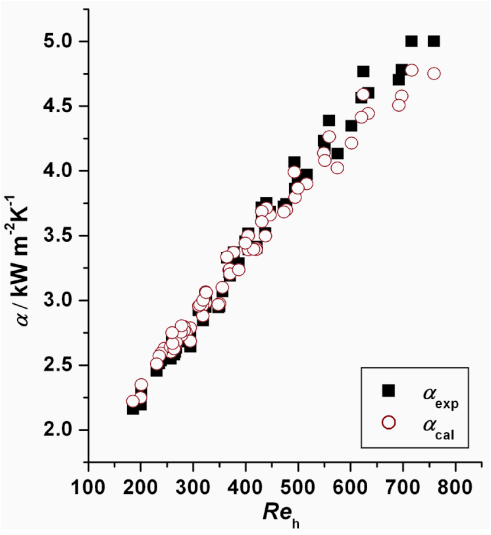

Fig. 3. Single phase water–ethylene–glycol heat transfer coefficient.

The influences of the mass flux of the refrigerant and the imposed heat flux on the heat transfer during evaporation are now closely analyzed. Selected data are shown in Fig. 4, which shows the dependence of heat transfer coefficient on

vapor quality for four different mass fluxes. It can be noticed that the heat transfer coefficient increases with the vapor quality, at least for the presented range of values. This tendency could be explained by the fact that with higher vapor quality, the thickness of liquid film decreases, and since this film represents an additional resistance to heat transfer, the influence on the heat transfer coefficient becomes favorable.

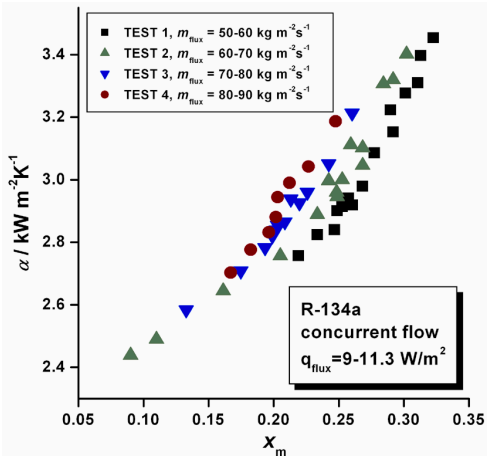

Fig. 4. Influence of mass flux on the heat transfer coefficient, concurrent flow.

The results shown in Fig. 4 for the four investigated mass fluxes during concurrent flow, indicate that the heat transfer coefficient rises with increasing mass flux. This is the consequence of the fact that a higher mass flux also means a higher velocity of the two-phase flow and better heat transfer. A similar tendency can also be noticed in the case of countercurrent flow (Fig. 5), which suggests that the convective boiling regime is dominant.

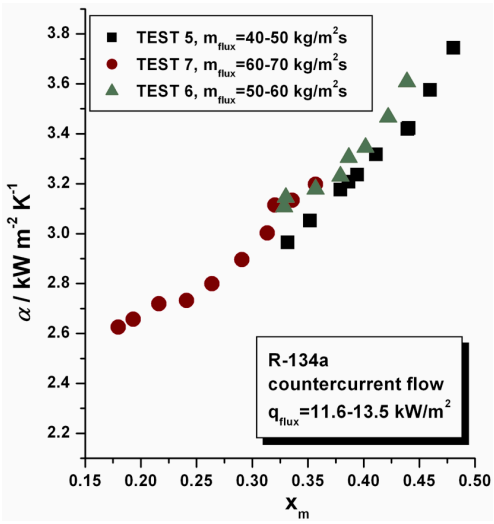

Fig. 5. Influence of mass flux on the heat transfer coefficient, countercurrent flow.

The effects of heat flux on the heat transfer coefficient are shown in Fig. 6. Two heat fluxes are compared under the same conditions of mass flux, system pressure and flow direction. The increase in heat flux induces a rise in heat transfer coefficient, although the effect seems to be less significant than that of mass flux. Such a behavior would indicate a dominance of the nucleate boiling regime.

The final conclusion could be that since the presented values of heat transfer coefficient are the mean values for the whole heat exchanger, both mechanisms occur along the plate and each of them is dominant in one section of the plate.

When the influence of flow direction on heat transfer is considered, under the same conditions of mass flux, heat flux and system pressure, the experiments showed that the heat transfer coefficients for concurrent flow are higher than in the case of countercurrent flow. This tendency, shown in Fig. 7, could be explained by the fact that in concurrent flow, temperature difference in the first part of the plate is higher than in the case of countercurrent flow. As a result, nucleate boiling, which is characterized by high heat transfer coefficients, occurs faster and better heat transfer is to be expected.

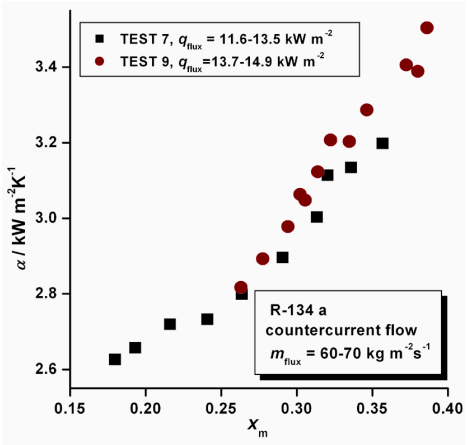

Fig. 6. Influence of heat flux on the heat transfer coefficient.

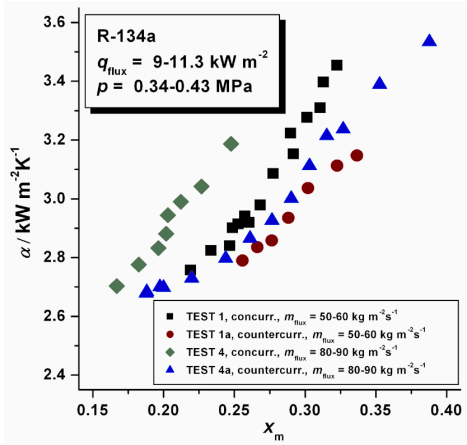

Fig. 7. Influence of flow direction on the heat transfer coefficient.

The results of a series of measurements under various experimental conditions are compared with the literature values[1] and presented in Fig. 8. These previously measured data correspond to experiments conducted with the same refrigerant, but under different test conditions and on a plate heat exchanger of different geometry (120 mm × 45 mm, with three single plates, forming two flow channels, one for each fluid).

Another comparison of the experimental data presented in this study with values calculated from literature correlations is given in Fig. 9.

The results marked with VDI and Martin were calculated from Eq. (7), with the value of the single-phase heat transfer coefficient calculated by different cor-

relations available in the literature.[20,21] The results labeled as Danilova and Steiner were directly calculated from the equation for the heat transfer coefficient during evaporation suggested by these authors.[9,22]

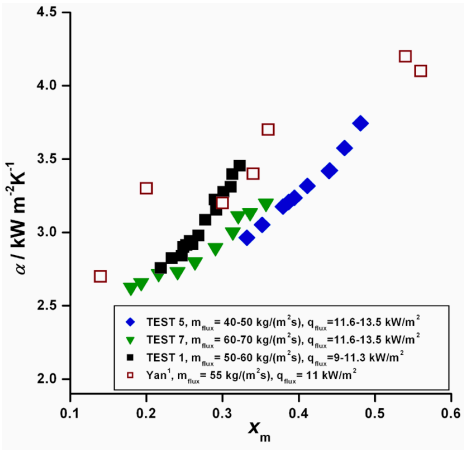

Fig. 8. Comparison with previous experimental data.[3]

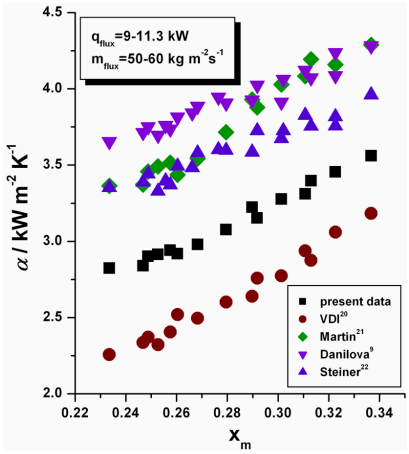

Fig. 9. Comparison of the current experimental data with correlations from the literature.

CONCLUSIONS

The results presented in this study show that all the analyzed factors, *i.e.*, mass flux, heat flux and flow configuration, influence, to some extent, the heat transfer coefficient during the process of evaporation. Since both mass flux and heat flux cause an increase in the heat transfer coefficient, it could be concluded that the boiling regime changes from nucleate boiling to convective boiling along the plate. The mean value of heat transfer coefficient given in this study would thus include the influence of both evaporation mechanisms. In order to determine in which section of the plate the dominate boiling regime changes from nucleate to convective; measurements of the local temperatures along the plate were undertaken. The collected data will enable the calculation of quasi-local heat transfer coefficients and give a better insight into the boiling process, which will be the subject of a future study.

Acknowledgement: The experimental measurements presented in this study were conducted in the Laboratory of the Institute of Thermodynamics at the Helmut Schmidt University of the Federal Armed Forces in Hamburg, Germany.

NOTATIONS

A – Heat transfer area, m^2
a – Amplitude of plate corrugation, m
B – Width, m
c_p – Specific heat, J kg^{-1} K^{-1}
D_h – Hydraulic diameter, m

L – Length, m
m – Mass flow rate, kg s^{-1}
m_{flux} – Mass flux, kg $m^{-2}s^{-1}$
N – Number of cassettes
Nu – Nusselt number
p^{sat} – Saturation pressure, Pa
Pr – Prandtl number
Q – Total heat transfer rate, W
q – Heat flux in one segment from the water mixture side, W m^{-2}
Re – Reynolds number
T – Temperature, °C
T^{sat} – Saturation temperature, °C
U – Overall heat transfer coefficient, W m^{-2} K^{-1}
u – Velocity, m s^{-1}
x_m – Mean vapor quality
u_m – Mean flow velocity, m s^{-1}

Greek letters

α – Heat transfer coefficient, W m^{-2} K^{-1}
δ_p – Thickness of the plate, m
Δh_v – Enthalpy of vaporization, J kg^{-1}
ΔT_{lmtd} – Logarithmic mean temperature difference, °C
Φ – Area enhancement factor due to corrugation
λ – Wave length of plate corrugation, m
λ_h – Thermal conductivity of hot fluid mixture, W/mK
λ_p – Thermal conductivity of plate material, W m^{-1} K^{-1}
μ – Viscosity, Pa s
ρ – Density, kg m^{-3}
ψ – Angle of plate corrugation, deg

Subscripts

ch – Channel
i – Inlet
h – Hot water–glycol mixture
o – Outlet
p – Plate
r – Refrigerant

И З В О Д

СРЕДЊИ КОЕФИЦИЈЕНТ ПРЕЛАЗА ТОПЛОТЕ ПРИ ИСПАРАВАЊУ 1,1,1,2-ТЕТРАФЛУОРЕТАНА (Р-134а) У ПЛОЧАСТОМ РАЗМЕЊИВАЧУ ТОПЛОТЕ

ЕМИЛА ЂОРЂЕВИЋ[1], STEPHAN KABELAC[2] и СЛОБОДАН ШЕРБАНОВИЋ[1]

[1]Технолошко–металуршки факултет, Универзитет у Београду, Карнегијева 4, 11120 Београд и [2]Helmut Schmidt University of Federal Armed Forces,Holstenhofweg 85, D–22043 Hamburg, Germany

У овом раду је експериментално истраживан коефицијент прелаза топлоте при двофазном току расхладног флуида 1,1,1,2-тетрафлуороетана (R-134a) у вертикалном плочастом размењивачу топлоте. Резултати су представљени као зависност средњег коефицијента прелаза топлоте за цео апарат од средњег степена сувоће x_m. Утицаји масеног флукса, топлотног

флукса и конфигурације тока флуида на коефицијент прелаза топлоте су такође узети у обзир а направљено је и поређење са предходно објављеним експерименталним подацима и корелацијама из литературе.

(Примљено 8. фебруара 2007)

REFERENCES

1. Y. Y. Yan, T. F. Lin, *ASME J. Heat Transfer.* **121** (1999) 118
2. Y. Y. Yan, H. C. Lio, T. F. Lin, *Intern. J. Heat Mass Transfer* **42** (1999) 993
3. Y. Y. Hsieh, L. J. Chiang, T. F. Lin, *Intern. J. Heat Mass Transfer* **45** (2002) 1791
4. Y. Y. Hsieh, T. F. Lin, *ASME J. Heat Transfer* **125** (2003) 852
5. W. S. Kuo, Y. M. Lie, Y. Y. Hsieh, T. F. Lin, *Intern. J. Heat Mass Transfer* **48** (2005) 5205
6. Y. Y. Hsieh, T. F. Lin, *Intern. J. Heat Mass Transfer* **45** (2002) 1033
7. D. Sterner, B. Sunden, *Heat Transfer Engin.* **27** (2006) 45
8. G. A. Longo, A. Gasparella, R. Sartori, *Intern. J. Heat Mass Transfer* **47** (2004) 4125
9. D. N. Danilova et al., *Kholodilnaya Tekhnika* **4** (1981) 25
10. L. M. Schlager, M. B. Pate, A. E. Bergles, *Intern. J. Refrigeration* **12** (1989) 6
11. L. M. Schlager, M. B. Pate, A. E. Bergles, *ASME J. Heat Transfer* **112** (1990) 1041
12. W. Xiaomin, W. Xiaoling, W. Weicheng, *J. Enhanced Heat Transfer* **11** (2004) 275
13. S. J. Eckels, M. B. Pate, *Intern. J. Refrigeration* **14** (1991) 70
14. T. Ebisu, K. Torikoshi, *ASHRAE Transcript.* **121** (1998) 556
15. K. Torikoshi, T. Ebisu, *ASHRAE Transcriptions* **99** (1993) 90
16. M. Andre, *Heat Transfer by the evaporation of NH_3 in a plate heat exchanger*, PhD Thesis (in German), Hannover University, Germany, 2004
17. S. J. Kline, F. A. McClintock, *Mechan. Engin.* **75** (1953) 3
18. E. Djordjević, S. Kabelac, S. Šerbanović, *5th International Conference of the Chemical Societies of the South-East European Countries*, Ohrid, Macedonia, *Proceedings*, 2006, p. 218
19. M. O. McLinden, S. A. Klein, E. W. Lemmon, A. P. Peskin, *NIST thermodynamic and transport properties of refrigerant mixtures – REFPROP*, Version 6.0, NIST, Boulder, 1998
20. H. Martin in *VDI – Wärmeatlas*, Springer Verlag, Heidelberg, 2002, p. Mm1
21. H. Martin, *Chem. Eng. Proc.* **35** (1996) 301
22. D. Steiner in *VDI – Wärmeatlas*, Springer Verlag, Heidelberg, 2002, p. Hbb1
23. S. Wellsandt, *Heat transfer and pressure drop in a plate type evaporator,* PhD Thesis, Chalmers University of Technology, Gothenburg, Sweden, 2001.